ISBN: 978-3-95450-211-0 doi:10.18429/JACoW-SRF2019-THP089

DEVELOPMENT OF SUPERCONDUCTING RF DOUBLE SPOKE CAVITY AT IHEP*

Z.Q. Quan†, F.S. He, W.M. Pan, Institute of High Energy Physics, 100049, Beijing, China

Abstract

The China Spallation Neutron Source (CSNS) is designed to produce spallation neutrons. CSNS upgrade is planned to increase beam power by inserting a SRF linac after drift tube linac (DTL). IHEP is developing a 325 MHz double spoke cavity at β0 of 0.5 for the CSNS SRF linac. The cavity shape was optimized to minimize Ep/Ea while keeping Bp/Ep reasonably low. Meanwhile, mechanical design was applied to check stress, Lorentz force detuning and microphonic effects, and to minimize pressure sensitivity. A new RF coupling scheme was proposed to avoid electrons hitting directly on ceramic window. After fabrication and post processing of cavity, the cavity reached Bp of 120 mT at Eacc = 13.8 MV/m and Q0 = 1.72E10 under vertical test at 2K.

INTRODUCTION

The CSNS upgrade consists of a SRF proton linac. The SRF linac will accelerate peak proton beam of 40 mA up to 303 MeV, and double spoke cavity is adopted for the SRF linac medium β section.

Spoke cavity evolves from half-wave resonator (HWR) operating in TEM mode. Compared with HWR, Multi-gap structure is possible in spoke cavity, which saves longitudinal space and increase the real-estate gradient. Compared with elliptical cavity, the spoke structure has higher shunt impedance, meanwhile, it is mechanically more stable and exhibit a stable field profile due to the high cell-to-cell coupling [1]. Thus double spoke cavity is a preferred candidate for medium β application.

ELECTROMAGNETIC DESIGN

Electromagnetic design includes geometry optimization, coupling port design.

Geometry Optimization

The cavity geometry is optimized to achieve maximum accelerating gradient (Eacc) during operation. One limit to the performance of a superconducting cavity is field emission (FE) at where surface electric field is high; another limit is quenching at where surface magnetic field is high. So the peak surface field to gradient ratio, i.e. Ep/Eacc and Bp/Eacc, are the major figure of merits for geometry optimization.

Based on the experience of previous ADS project, SRF cavities seldom quench below Bp of 90mT; though, FE may occur at Ep as low as 35 MV/m, and the degradation of FE onset is observed over some time of beam operation. So the main optimization target is to reduce Ep/Eacc, while the Bp/Ep is kept below 2.57 mT/(MV/m).

The Ep/Eacc is most sensitive to the central part of the spoke and the end-cover cone shape, i.e. T_k, S_{gl}, S_{al}, and S_{bl}, as shown Fig. 1. The base of the spoke has more influence on Bp/Eacc, and it is biased to a racetrack shape in order to further reduce Ep/Eacc [2]. The major geometry parameters optimized are shown in Fig. 1. The final cavity length C_l is 729 mm, and the cavity diameter C_d is 560 mm.

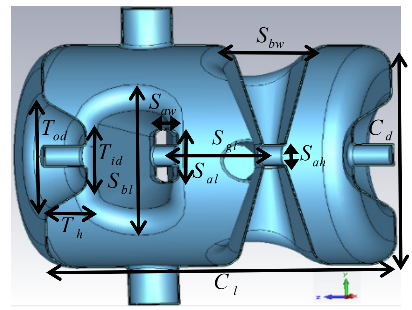

Figure 1: Parameters for optimization.

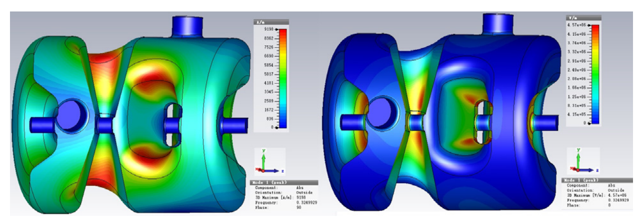

H-field distribution E-field distribution

Figure 2: Electromagnetic field distribution of double spoke cavity.

After optimization, Ep/Eacc achieved 3.4, and the Bp/Eacc is 8.7 mT/(MV/m); in case the cavity is operated with Ep of 35 MV/m, then the Bp is 90mT, and the gradient can reach 10.3 MV/m, which is higher than the project target of 7.3 MV/m. The surface field profile of the cavity is shown in Fig. 2, while detailed design parameters are listed in Table 1.

Table 1: The Major Parameters of Double Spoke Cavity

Description	Results
Frequency (MHz)	325
R-aperture (mm)	50
Epk/Eacc	3.4
Bpk/Eacc (mT/(MV/m))	8.67
G*R/Q (Ω^2)	5.08e4
df/dP (Hz/mbar)	3.35
LFD factor (Hz/(MV/m)^2)	-10.9
Tuning sensitivity (kHz/mm)	93
Cavity rigidity (kHz/kN)	16.78

*Work supported by the State Key Development Program for Basic Research of China (Grant No. 2014CB845500)
†zhouquan@ihep.ac.cn

ISBN: 978-3-95450-211-0 doi:10.18429/JACoW-SRF2019-THP089

Coupling Port Design

Three issues have been considered for the coupling port design.

First, it is important to avoid the FE electrons, which are generated on cavity inner surface, hitting the ceramic window of the coupler. Here a 30 degree bending is applied to the coupling port, so the ceramic window will not see the high electric field region on the spoke centre. The bending angle and the antenna length are carefully checked, to make sure that there is space to insert the antenna into the coupling port.

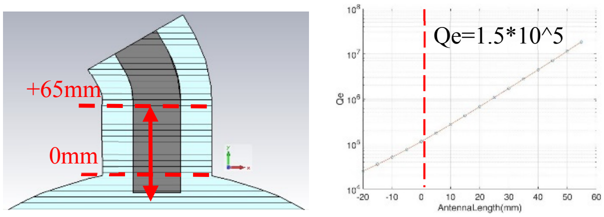

Figure 3: Winding coupling port & Qe versus antenna length.

Second, antenna length is selected to reach desired Qe. Assuming the cavity operates at 9 MV/m with 10-100 mA proton beam, then the matched Qe is 1.5e5-1.5e6 by using Eq. (1) [1]. By calculating the Qe vs the antenna length of a 50Ω coaxial line, it is found that the antenna tip is 3mm away from cavity inner surface at the minimum Qe, which is shown in Fig. 3.

When $P_b \gg P_c$

$$Q_e \approx \frac{Q_0}{P_b/P_c} = \frac{V_c}{I_b/(R_a/Q_0)} \tag{1}$$

Third, the heat load on the blank flanges should be low, in order to measure the cavity Q_0 accurately during vertical test. The total Q induced by 6 flanges is above 4e11, by properly choosing the length of the coupling port and material of blank flanges.

MECHANICAL DESIGN

Mechanical performance of the cavity was optimized with COMSOL. The simulation results are listed in Table 1 in the last page.

There are three design targets. The first is to minimize He pressure sensitivity (df/dp); the second is to make sure the cavity will not plastically deform in any possible boundary condition during post processing, testing, and operation; the third is to make sure the lowest intrinsic vibration frequency is above 100 Hz.

Pressure Sensitivity

The structure of the cavity is shown in Fig. 4. The cavity helium vessel is made of Ti, and the cavity end-cover is connected with the helium vessel by a Nb55Ti ring. Nb ribs inside the spoke are used to reduce df/dp and stress. For naked cavity, Ti blocks on end-cover are used to support the cavity with a fixture.

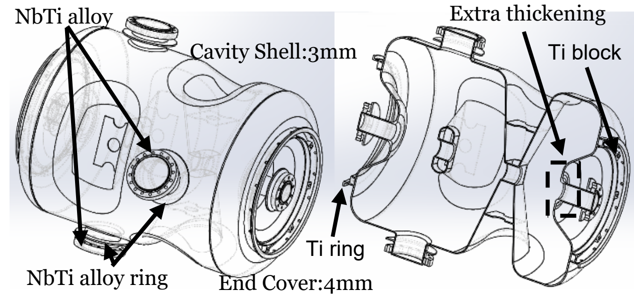

Figure 4: Mechanical design of double spoke cavity.

It is well known that geometry deformation will cause frequency deviation, and the frequency change can be calculated by Slater's theorem [i.e., Eq. (2)]. When the cavity beam port is free, the frequency deviation induced by pressure change inside the helium vessel is balanced by properly placing the stiffening rings and ribs. A df/dp of 3.35 Hz/mbar is achieved, and Fig. 5 illustrate that the frequency change induced by electric field and magnetic field dominated zone cancel each other.

$$df \propto (\varepsilon_0 E^2 - \mu_0 H^2) dV \tag{2}$$

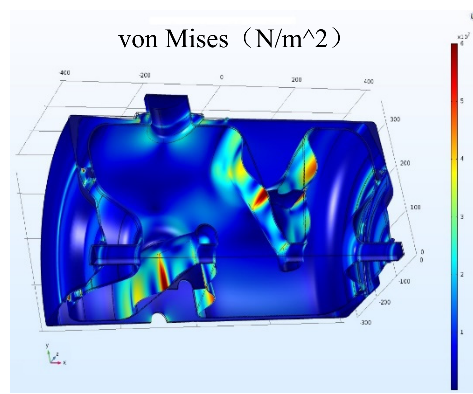

Figure 5: Stress & deformation(×100) with beam pipe free.

Stress Analyses

There are typically three different boundary conditions to be analysed, as shown in Fig. 6 and Table 2. The maximum stress on the cavity wall occurs at the boundary condition of leak check, which is shown in Fig. 7, and it is still below the allowable stress of 47 MPa [3]. For naked cavity, the fixture hold the stiffening ring on end-cover, and the stress is below allowable stress too.

Table 2: Boundary Conditions for Stress Analyses

	In	HeV*	Out	BP*
Leak check	Vac.	1 atm	1 atm	Free
Cooling down	Vac.	1 atm	Vac.	Free
Tuning(4K)	Vac.	1 atm	Vac.	Free+Push

*HeV is short for helium vessel, and BP is for beam pipe

ISBN: 978-3-95450-211-0 doi:10.18429/JACoW-SRF2019-THP089

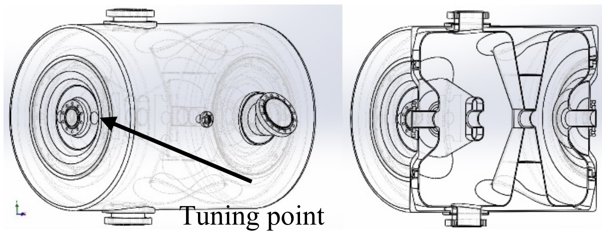

Figure 6: Double spoke cavity with helium vessel.

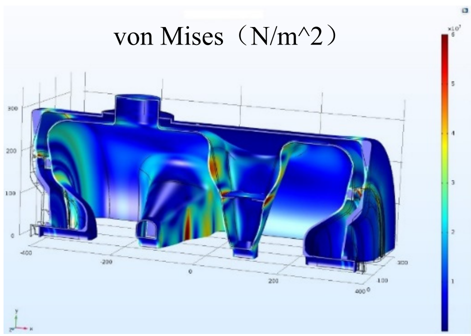

Figure 7: Surface von Mises stress of leakage detecting& Displacement(×50).

Tuning Sensitivity

The tuning force is applied on a single side of the cavity near the beam pipe, as shown in Fig. 6, and the displacement by pushing the end-cover is defined as positive. The stress and displacement are simulated at various tuning force, and it is found that the stress on cavity is smaller when pushing the cavity compared with pulling, as shown in Fig. 8.

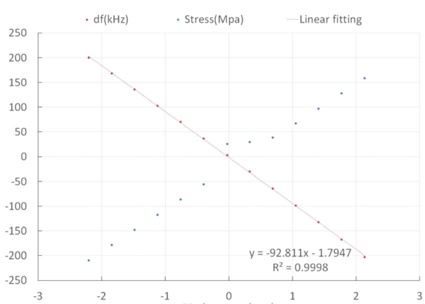

Figure 8: Stress and freq. change vs tuning force.

Lorentz Force Detuning

The interaction of the cavity field with the induced surface currents and charges results in an electromagnetic surface forces in RF cavities [4]. The induced frequency shifting effect is called Lorentz force detuning (LFD), and it has to be considered and corrected by low level control system. The definition of LFD coefficient is as following:

$$K_L = \Delta f / E_{acc}^2 \tag{3}$$

Frequency shift at various gradient are simulated to fit the LFD coefficient, as shown in Fig. 9. The maximum deformation is located near the high electric field region, The K_L is-10.9 Hz/(MV/m)^2 with ports free

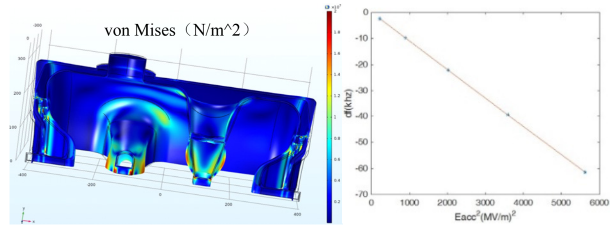

Figure 9: Displacement (×200) caused by Lorentz force@75MV/m(left) & LFD coefficient fitting(right).

Vibration Mode

The mechanical resonance modes are analysed with cavity beam pipe free and sitting on the center of its helium vessel. The lowest vibration frequency is 296 Hz, as shown in Fig. 10, indicating there is no danger of microphonic resonance.

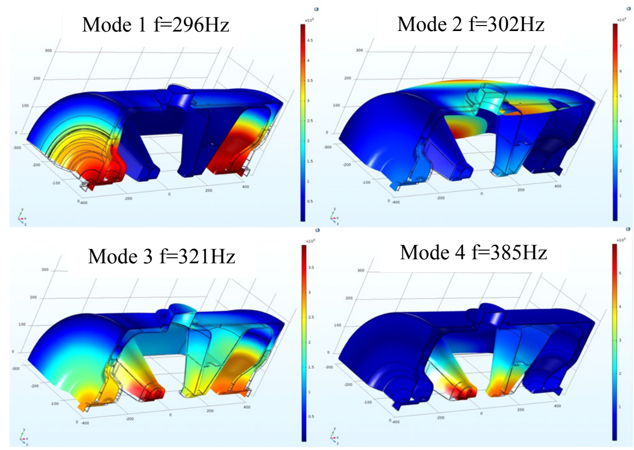

Figure 10: The lowest vibration modes.

FABRICATION

The cavity consists of three major components, which can be seen in Fig. 11. The end cover and half of Spoke were both stamp formed. The outer conductor of the cavity was rolled from a niobium sheet.

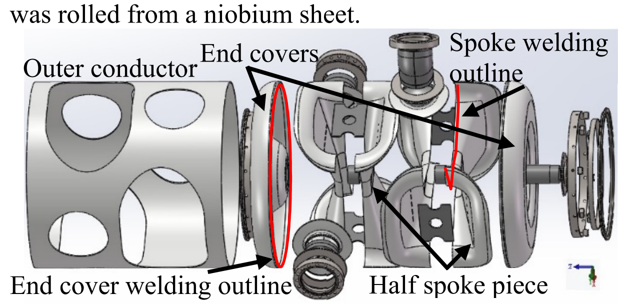

Figure 11: Fabrication parts of Double Spoke Cavity.

Fabrication Process

The outer conductor is made of a whole niobium piece by rolling. The length of the niobium sheet was calculated, so after rolling and Electron Beam Welding (EBW), the diameter of outer conductor is 560 mm. Seven ports were opened on the outer conductor, the dimensions of all ports were carefully measured and processed, so ports can match coupling and spoke parts properly.

ISBN: 978-3-95450-211-0 doi:10.18429/JACoW-SRF2019-THP089

Spoke was welded from two halve-spoke pieces. The racetrack blend of spoke base may easily be torn during the deep drawing, due to large distortion and extension. So annealed soft aluminium sheets with carefully trimmed shape were used to do the stamping tests. After stamping and machining, the thickness of the welding outline of half spoke piece (see Fig. 11) was no longer uniform.

The end cover was stamped as a whole piece, except for the the thicker piece around the beam pipe. After the stiffening ring welding, the end cover was deformed due to welding strength, so the welding outline of end cover connecting to outer conductor (see Fig. 11) had to be levelled, while the thickness of the wall was thinned to 3 mm thickness to match the thickness of outer conductor.

Welding Technology

There were three types of welding technology been used, electron beam welding(EBW) laser beam welding(LBW) and tungsten inert gas arc welding(TIG). EBW was used when welding niobium, LBW and TIG were used to weld niobium and Nb-Ti.

EBW requires gap along welding trajectory is less than 0.1mm to avoid melting through. Also welding beam voltage should be carefully chosen, since the thickness of the stamped parts are no longer uniform. Therefore parts dimension measurement and welding tests were done for each welding parameters.

Before assembling parts into welding tooling, all parts were ultrasonic cleaned, buffered chemical polished (BCP) by 6um, rinsed with deionized water and sealed in plastic bag for clean room. Cleaned parts were transported to class100 clean room to dry out.

Frequency Control

Before welding end covers with outer conductor, frequency of the cavity should be measured in standard ambient conditions (see table 3).

Table 3: Frequency Measurement in Room Temperature

Standard reference	Value
Temperature	20℃
Atmospheric pressure	101325Pa
Relative humidity	50%

For this cavity, frequency shift due to evacuation and cool down is -0.579 MHz [5], and frequency shift due to 180um BCP is calculated by perturbation method which is 0.183 MHz [6]. Taking 0.1 MHz as frequency shift of pre tuning system, frequency target after EBW in room temperature should be 324.704 MHz.

When trimming the outer conductor (see Fig. 12) to adjust the cavity frequency, both sides of the outer conductor should be trimmed equally to make sure the field profile is symmetric. Ep/Eacc and optimized beta were calculated, and they are not sensitive to cavity length. In this condition, the calculated and measured trimming sensitivity are both 80 kHz/mm.

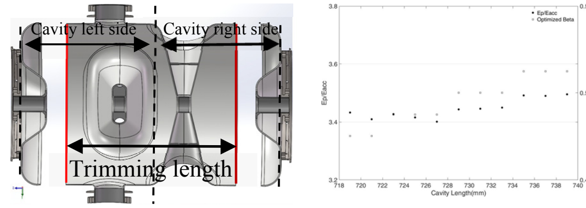

Figure 12: Fabrication tuning.

POST PROCESSING

The post processing procedure is shown in Fig. 13. Based on the experience of previous cavity surface treatment at IHEP, the microwave surface of Nb cavity should be removed 150 µm thickness at least.

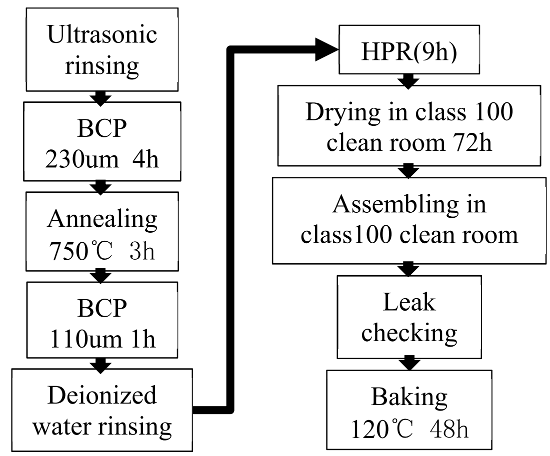

Figure 13: Cavity surface processing steps.

The BCP adopts the standard volume ratio of HF: HNO3: H3PO4 (1:1:2) acid mixture. To avoid Q-disease during BCP process, the acid temperature should not exceed 25℃. Acid came into the cavity through two ports on the bottom, and came out of the cavity from the top, as shown in Fig. 14. To ensure the uniformity of etching, the intake and venting ports should be reversed after 2h BCP.

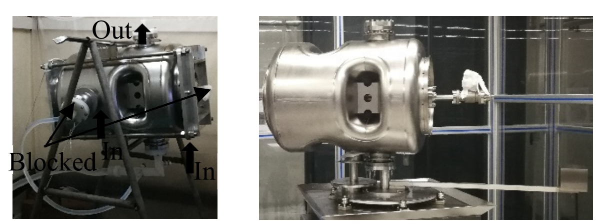

Figure 14: The BCP set-up of double spoke cavity (left) & HPR (right).

To avoid Q-disease from hydrogen absorbed by niobium surface during the BCP process, annealing after 4 h BCP was necessary. It took 30 minutes to evacuate the furnace so the vacuum is better than 1E-3Pa. then the furnace temperature rose from 30ºC to 750ºC in three hours; the furnace temperature was kept in 750ºC for 3 hours before cooling down to room temperature in vacuum.

To remove contamination in the high baking, the cavity was BCP treated for another hour, followed by deionized water rinsing of 30 minutes to make sure there was no residual acid inside cavity.

ISBN: 978-3-95450-211-0 doi:10.18429/JACoW-SRF2019-THP089

There are five ports on the cavity, and each port should be high pressure rinsed (HPR), as shown in Fig. 14. Each port was rinsed for 2 rounds with the nuzzle moving vertically at 30mm/min. The rotation speed of the cavity is 4 rounds per minute. To avoid contamination at the assembly stage, each port was sealed by the vertical test flange after HPR; there was only one port open for dry after the HPR, therefore a conservative drying time was used.

VERTICLE TEST RESULTS

The geometric factor of this cavity is 123 Ω, Bardeen-Cooper-Schrieffer (BCS) resistence under 2K was estimated to be 0.7 nΩ, taking 10 nΩ as resdiual resistence, the Q0 of this cavity under 2K is estimated to be 1E10. Therefore Qe of Pin for vertical test is designed to be 8E9.

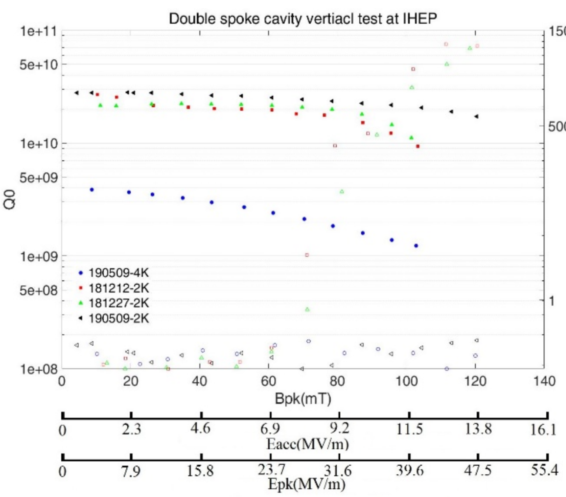

Figure 15: Vertical test results.

The cavity was tested for three times, overall test results can be seen in Fig. 15.

The first vertical test was conducted in December 12, 2018. It took 3 hours for multipacting processing, and severe multipacting occurred below 3 MV/m. Radiation rose from 6 MV/m and reached 14000 uSv/h at 11.9 MV/m and Q0 was 9.4E9

The cavity was high pressure rinsed again for 9h and re assembled in classs100 clean room. In December 27, 2018, the cavity was tested again under 2K, There was a slight improvement on Q0 and Radiation, it still quenched at 11.9 MV/m at Q0 = 1.05E10.

Due to the field emission from previous result, surface with high electric field (see Fig. 16) was polished by hand using electric grinding machine. Ultrasonic thickness gauge was used to make sure thickness of 30um-50um of material surface was removed by hand polishing. 600 mesh grinding wheel was used on a Niobium sample, before BCP the surface roughness Ra of sample grinded by 600 mesh grinding wheel is 360 nm, after 15 um BCP the Ra of Niobium sample is 420 nm. Therefore the roughness of microwave surface of cavity polished by 600 mesh grinding wheel do not have strong field emission under electric field of 175 MV/m[7].

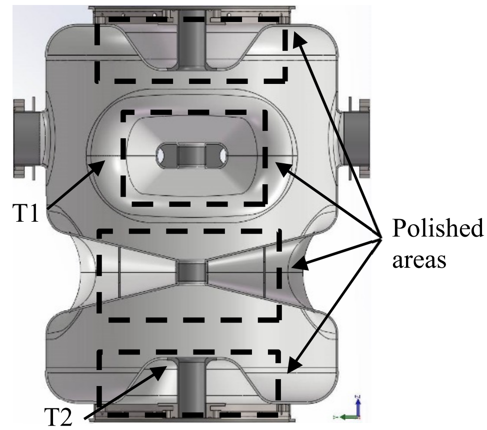

Figure 16: Strong electric surfaces.

After hand polishing, the cavity was ultrasonic cleaned and BCP treated for another 40minutes, and minimum removal of 25um was achieved to make sure there was no other substance embeded on the microwave surface. In May 9, 2019, the cavity was verticle tested on 2K and 4.2K, two temperature sensor was attached on the cavity outer surface (see Fig. 16). In 2K test, Bp of 120mT was reached when acceleration gradient is 13.8 MV/m at Q0 = 1.72E10. In 4K test, when acceleration gradient reached 11.8MV/m at Q0 = 1.24E9, the cavity performance was limited by the power source ; also when maitaining the acceleration gradient at 11.8 MV/m, temperatue rose significantly and finally exceed 9.2K at T2. In both 2K and 4K tests, there were no signifcant radiation, also MP at soft barriers under 3 MV/m are suppressed sifnificantly.

The Cavity reached Bp of 120 mT at highest acceleration gradient while ESS double spooke cavity Romea reached 104 mT and Giulietta reached 88mT [8]. IMP double spoke cavity reached 116 mT [9]. Assuming all cavities are runing at Eacc of 9MV/m, Ep of this cavity is 31 MV/m while Giulietta and Romea is 39 MV/m, IMP double spoke cavity is 34 MV/m. Compare with same type and similiar beta double spoke cavity around the world, the cavity reached same level of Bp, in the meantime, it has the lowest Ep at same acceleration gradient to avoid field emission.

CONCLUSION

The systematic design of the beta0.5 double spoke cavity has been accomplished, including RF parameters optimization, coupling port design, structure design, pressure sensitivity optimization, stress analysis, tuning simulation, LFD analysis, and vibration mode analysis.

The cavity was fabricated within 8 month and vertical tested three times under different surface treatment. In latest 2K vertical test, the cavity reached Eacc of 13.8 MV/m at Q0 = 1.72E10.

Now another surface treatment such as surface defect inspection in high-magnetic field region and barrel polishing is ongoing. After this round of surface treatment, the cavity is planned to vertical test again on September 2019.

ISBN: 978-3-95450-211-0 doi:10.18429/JACoW-SRF2019-THP089

REFERENCES

[1] Hasan Padamsee, *RF Superconductivity*. Cornell University, Ithaca, USA: VILEY-VCH Verlag GmbH & Co. KGaA, 2009.

[2] J. R. Delayen, S. U. De Silva, and C. S. Hopper, "Design of Superconducting Spoke Cavities for High-velocity Applications", in *Proc. 24th Particle Accelerator Conf. (PAC'11)*, New York, NY, USA, Mar.-Apr. 2011, paper TUP100, pp. 1024-1026.

[3] Xin-Yin Zhang et al., "Design of a 325MHz half wave resonator prototype at IHEP", *Chinese. Physics. C.*, vol. 40, NO. 8, Aug. 2016.

[4] E. Haebel and J. Tuckmantel, "Electromagnetic Surface Forces in RF Cavities", CERN, Geneva, Switzerland, CERN-AT-RF(Int)-91-99, Dec.1991.

[5] Frank Marhauser., "JLab SRF Cavity Fabrication Errors, Consequences and Lessons Learned", Jefferson Laboratory, 12000 Jefferson Avenue, VA, 23606. JLab-TN-10-021, Aug, 2010.

[6] David M. Pozar, Microwave Engineering. Jhon Wiley & Sons, Inc, 2005.

[7] S. Lagotzky, G. Mueller, A. Navitski, A. L. Prudnikava, and Y. Tamashevich, "Field Emission Investigation of Centrifugal-Barrel-Polished Nb Samples", in *Proc. SRF'15*, Whistler, Canada, Sep. 2015, paper MOPB059, pp. 237-241.

[8] H. Li, V.A. Goryashko, A. Bhattacharyya, R. Ruber, "RF Test of the ESS Double Spoke Cavity", Uppsala University, Uppsala, Sweden, FREIA Report 2016/1, Jan. 2016.

[9] Tiancai Jiang et al., "Design and test result of a superconducting double-spoke cavity", Nuclear Engineering and Technology, vol.51, pp. 877-883, 2019